First-principles study on nonlocal ferromagnetism in (Cu, N)-codoped ZnO*

Qin Guo-Ping(秦国平)[a)b)], Wang Xin-Qiang(王新强)[a)†], Zheng Ji(郑 继)[a)], Kong Chun-Yang(孔春阳)[b)], Ruan Hai-Bo(阮海波)[a)], Li Wan-Jun(李万俊)[a)], Zhao Yong-Hong(赵永红)[b)], and Meng Xiang-Dan(孟祥丹)[b)]

[a)] *College of Physics, Chongqing University, Chongqing* 400030, *China*

[b)] *Key Laboratory of Optoelectronic Functional Materials, Chongqing Normal University, Chongqing* 400047, *China*

(Received 9 July 2012; revised manuscript received 26 December 2012)

First-principles calculations based on spin density functional theory are performed to study the spin-resolved electronic properties of ZnO codoped with Cu and N. (Cu, N)-codoped ZnO exhibits magnetism, and the total magnetic moment mainly originates from the p–d hybridization of Cu–N and Cu–O as well as p–p coupling interaction between N and O at the Fermi level. The $Zn_{34}Cu_2O_{35}N_1$ favors energetically a ferromagnetic ground state due to the existence of stable Cu–N–Cu complex. These results imply that the (Cu, N)-codoped ZnO is a promising dilute magnetic semiconductor free of magnetic precipitates, which could broaden the horizon of currently known magnetic systems.

Keywords: nonmagnetic impurity, hybridization, ferromagnetism, first-principles study

PACS: 71.15.Mb, 71.20.Nr, 71.55.Gs, 75.50.Pp **DOI:** 10.1088/1674-1056/22/5/057101

1. Introduction

Diamond ZnO has been actively studied as a promising diluted magnetic semiconductor (DMS) for realizing ferromagnetism with high Curie temperature (T_C).[1,2] Many research groups have investigated the spin-resolved electronic properties of ZnO doped with transition metals (TM, e.g., Sc,[3] Ti,[4] V,[5] Cr,[6] Mn,[7] Fe,[8] Co,[9] and Ni[10]) or rare earth elements (REE, e.g., Eu[11]). Theoretical calculations predicted that ZnO-based DMSs doped with V, Cr, Fe, or Ni show high-T_C ferromagnetism.[12] It was also found that Mn-doped ZnO changes its magnetic state from an antiferromagnetic (AFM) one to a ferromagnetic (FM) one with the increase in the hole concentration.[13–15]

Though ferromagnetism at up to room temperature or even higher has been reported experimentally, and the mechanisms of ferromagnetism in DMS materials, such as double exchange, super-exchange Ruderman–Kittel–Kasuya–Yosida (RKKY) type, and bound magnetic polaron (BMP), have been proposed, inconsistent magnetic properties for TM-doped ZnO ranging from spin glass and paramagnetic behaviors to FM have been reported by different groups. For instance, the Co-doped ZnO changes its magnetic state from the AFM state to the FM state without and with the defects.[16] Moreover, the FM in TM-doped ZnO systems may result from the precipitation of TM impurities which are undesirable for practical applications. Therefore, the origin of the intrinsic FM involved has not been confirmed yet.

To solve the problems mentioned above, nonmagnetic ion-doped ZnO can provide a possible approach for exploring new areas of ZnO-based DMSs. Pan and Yi[17] reported that the magnetic moment is in a range of 1.5–3.0 μ_B/C for all the C-doped samples, and hole doping can enhance ferromagnetism. Though first-principles calculations showed that Cu-doped ZnO favors a spin polarization and a ferromagnetism ground state, there is discrepancy on whether n-type or p-type is beneficial to the ferromagnetism in the ZnO:Cu sample. Herng *et al*.[18] observed RT ferromagnetism in ZnO:Cu film with the coexistence of 2 at.% Cu doping and 1 at.% (or less) Vo under optimal conditions, while the Cu/Al codoping experiments[19] suggested that additional carriers suppress the FM order by occupying the vacant Cu 3d states. Additionally, N is a promising candidate for the p-type doping of ZnO, and Shen *et al*.[20] and Shi *et al*.[21] predicted that ZnO doped with N has magnetic properties of long-range FM coupling. So far, the key questions on the microscopic mechanism of the reaction are still open. In this paper, we explore in detail the origin of the intrinsic ferromagnetism in the (Cu, N)-codoped ZnO system by first-principles calculations based on spin density functional theory.

2. Method and model

The total energy and electronic structure calculations are carried out in a supercell of ZnO with wurtzite structure, as implemented in the VASP code.[22] The exchange and correlation functionals are treated under the generalized gradient approximation (GGA) of Perdew–Burke–Ernzerhof

*Project supported by the National Natural Science Foundation of China (Grant No. 61274128), the Natural Science Foundation of Chongqing City, China (Grant Nos. 2011BA4031 and 2013jjB0023), the Education Commission of Chongqing City, China (Grant No. KJ120608), and the Chongqing Normal University, China (Grant No. 09XLS04).

†Corresponding author. E-mail: xqwang@cqu.edu.cn

© 2013 Chinese Physical Society and IOP Publishing Ltd

(PBE).[23] The lattice constants are optimized and obtained as $a = b = 3.249$ Å and $c = 5.205$ Å ($c/a = 1.602$), which are in good agreement with experimental values.[24] In view of the projector-augmented plane wave (PAW) potentials, the valance electrons for Zn, O, Cu, and N are chosen to be $3d^{10}4s^2$, $2s^22p^4$, $3d^{10}4s^1$, and $2s^22p^3$ in a reciprocal space, respectively. Brillouin zone integrations are performed with the $4\times4\times4$ Γ centered K-point grid to make sure the total energy is relatively stable. The cutoff energy of plane waves which expand the wave functions as well as the maximum force are set to be 400 eV and 0.02 eV/Å, respectively. Meanwhile, self-consistency is considered not to be achieved until the difference in energy of a single atom between succeeding iterations is less than 1×10^{-5} eV per atom.

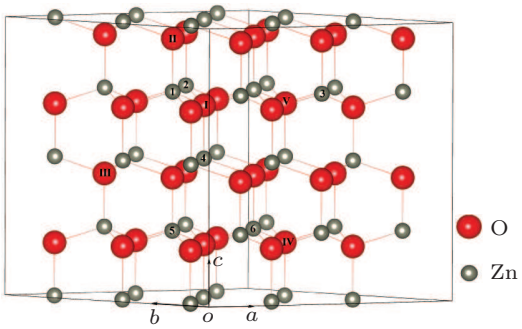


Fig. 1. (color online) The 72-ion supercell ZnO structure. The big (red) and small (grey) balls denote O sites and Zn sites, respectively.

3. Results and discussion

Firstly, we perform systematical calculations on the $Zn_{34}Cu_2O_{36}$ supercell corresponding to a Cu concentration of 5.6%. As shown in Fig. 1, several doped configurations are constructed according to the order of Cu–Cu separation. The number (1-i) is defined as a doped Cu pair, where one Cu substitutes Zn site labeled as "1", and the other Cu substitutes Zn site labeled as "i" ($i = 2$, 3, 4, 5, 6). The energies of FM, AFM phase relative to that of configuration (1–4) are listed in Table 1. It shows that all the configurations mentioned above favor the FM ground state, especially the configurations 1–4 with Cu pairs closely along the c axis. In addition, the total magnetic moment is always $1.82\mu_B$ per supercell in all configurations with the FM ordering. Here, the local moment at Cu is about $0.56\mu_B$ and the remaining magnetic moment mainly arises from the spin-polarized O. It is confirmed that spontaneous spin polarization mainly originates from the p–d exchange interaction between Cu 3d and its four neighboring O 2p orbitals in the tetrahedron. Remarkably, the stabilization of the FM is also related to the d–d coupling between Cu atoms (often denoted as double exchange), which can lower the energy of the partly occupied minority t_{2d} state of Cu.

Table 1. Total energies of the FM and AFM phase in different configurations calculated with respect to that with lowest FM energy in the $Zn_{34}Cu_2O_{36}$ supercell. $\Delta E = E_{FM} - E_{AFM}$ is defined (per supercell) for determining the magnetic stability ($\Delta E < 0$ indicates favorable FM). M_{Cu} denotes the magnetic moment on each of the two Cu atoms.

Site (Cu–Cu)	E_{FM}/meV	E_{AFM}/meV	ΔE/meV	M_{FM}/μ_B
(1–2)	10	174	–164	0.56/0.56
(1–4)	0	340	–340	0.56/0.56
(1–3)	270	340	–70	0.56/0.56
(1–5)	334	454	–120	0.57/0.57
(1–6)	290	338	–48	0.56/0.56

Then, we study the properties of nonmagnetic ions N-doped ZnO. One anionic O is substituted by N in the 72-ion supercell, and the total energies of both spin-polarized and spin-unpolarized states are calculated. It is found that the N-doped ZnO favors energetically the spin-polarized state, and its total energy is 24 meV lower than that of the nonspin-polarized state, which accords with previous calculation in the main features.[20] In addition, almost all magnetic moments ($0.65\mu_B$ per supercell) reside on the p states of anionic N and its neighboring anionic O within the distance of about 3.25 Å, indicating that the coupling between those 2p states has a large spatial extension.

In the following, to clarify the effect of the anionic N codoping on the magnetic moment of Cu-doped ZnO, we investigate magnetic exchange interaction between Cu_{Zn} and No with a separation distance in the $Zn_{35}Cu_1O_{35}N_1$ supercell. The values of m and n represent different doping configurations, and m and n mean that the Zn_m and O_n are replaced by Cu and N, respectively. It is found that the No defect prefers to be attached to the Cu dopant in the tetrahedron with a length of Cu–N bond (1.857 Å), less than that of Zn-O (1.973–1.980 Å) or Cu–O (1.985 Å), and its total energy is at least 490 meV lower than that of N_O outside of the CuO_4 tetrahedron in the $Zn_{35}Cu_1O_{35}N_1$ supercell. Next, the total magnetic moment of $Zn_{31}Cu_1O_{31}N_1$ ($1.64\mu_B$) is slightly less than that of $Zn_{34}Cu_2O_{36}$ supercells ($1.82\mu_B$). The defect formation energy is given by

$$E^f(D) = E_{tot}(D) - E_{tot}(ZnO) + \sum n_i\mu_i,$$

where $E_{tot}(D)$ and $E_{tot}(ZnO)$ are respectively the total energies of the defective and perfect supercells, and n_i and μ_i are the changes in number and the chemical potential of species i, respectively.[25] The defect formation energy of Cu_{Zn}+No in the $Zn_{35}Cu_1O_{35}N_1$ supercell is 2.76 eV lower than that of Cu_{Zn}+Cu_{Zn} in the $Zn_{34}Cu_2O_{36}$ supercell in O-poor conditions.

Figure 2 shows the total and partial densities of state (DOSs) for magnetic $Zn_{35}Cu_1O_{35}N_1$ in some configurations. The Fermi energy is located at the top of the valence band. The electronic structure shows a half-metallic characteristic, and thus the valence electrons at the Fermi level are almost 100% spin polarized (Fig. 2(a)). In Fig. 2(b), it is apparent

that the dopant Cu 3d state couples strongly with the dopant No 2p state which bonds to Cu near the Fermi level, referred to as p–d hybridization. This dominating hybridization results in the significant promotion of the spin-down densities of Cu 3d and N 2p states near the Fermi level, inducing the broad sub-bands and a delocalized distribution. Once Cu_{Zn} and No are separated by other ions, we conclude that their exchange interaction is slight. Moreover, on-site Coulomb repulsion U is taken into account as a result of the strong correlation effect of Cu 3d states ($U = 7$ eV for Zn and 3 eV for Cu).[19] It can be seen in Fig. 2(d) that the band gap energy calculated using the GGA+U is larger than that using the GGA (Fig. 2(d)), while their total magnetic moments are comparable due to the similar overlap between Cu 3d and N 2p states (Fig. 2(e)).

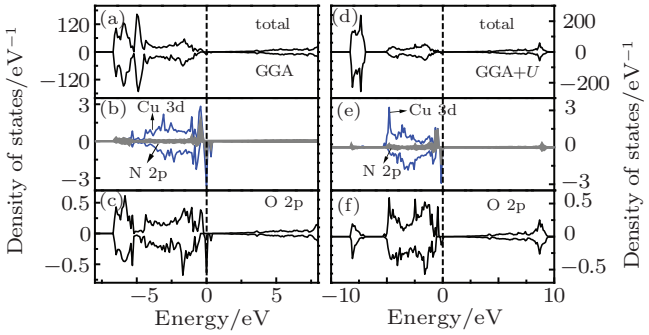


Fig. 2. (color online) (a) Total density of state (DOS) for (Cu, N)-codoped ZnO with the configuration (1, II). The supercell consists of eight (3×3×2) primitive cells of ZnO, where one Zn ion is substituted by Cu and one O ion by N. (b) Partial DOS of N 2p and Cu 3d. (c) Partial DOS of O 2p. Panels (d)–(f) represent the corresponding results using GGA+U. Fermi level is set to be 0 eV and indicated by the dotted vertical line.

Additionally, the magnetism partially results from the p–d exchange interaction between Cu 3d and its three other neighboring O 2p orbitals in the tetrahedron (Figs. 2(c) and 2(f)), similar to that of Cu-doped ZnO. Meanwhile, in terms of the isosurface of the spin distribution (Fig. 3), we also find that there exists a long range weak magnetic coupling between anionic N 2p and its neighboring anionic O 2p, which in turn enhances the spin polarization of cationic Cu. In particular, since No is far from the CuO_4 tetrahedron, the local magnetic moment of N decreases by 53.6% and the corresponding total magnetic moment per supercell varies slightly (1.63±0.01 μ_B). It is easily understood that there is an enhancement of the p–p coupling interaction due to longer bond length (1.948 Å) and weak covalency of Zn–N with respect to that of Cu–N based on Mulliken bond population analysis. Therefore, the total magnetic moment originates from the coexistence of the p–d hybridization of Cu–N or Cu–O and p–p coupling interaction between the N 2p and O 2p states at the Fermi level.

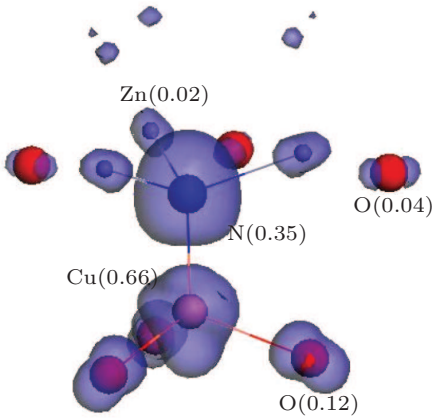


Fig. 3. (color online) Isosurface of the spin distribution surrounding the bond of Cu–N. Magnetic moment (μ_B) of each atom is given in parentheses.

Finally, in order to further ascertain a clear picture on the magnetic property in (Cu, N)-codoped ZnO, we also perform the calculations on electronic spin alignment of Cu fixed in parallel (FM state) and antiparallel (AFM state) manners, respectively, for all geometrically possible configurations consisting of two Cu and one N in a 3×3×2 ZnO supercell. The (m–i, n) denotes different doping configurations, where m and i mean that two sites of Zn are substituted by Cu. Meanwhile, n means that the O site labeled with n is replaced by N. Figure 4 shows the energies of various configurations considered with respect to that of the configuration (1–2, I) with FM ordering and the energy difference between FM and AFM ordering, $\Delta E = E_{FM} - E_{AFM}$ (the energy difference defined per supercell) for determining the magnetic stability. As a result, all configurations energetically favor parallel alignment of the local spin moments, with a total magnetic moment of 2.53μ_B. Obviously, there is a strong tendency toward the formation of complexes consisting of two Cu ions and one N ion which occupies the nearest sites of the Cu dopant such as the stable configurations (1–2, I) and (2–4, I).

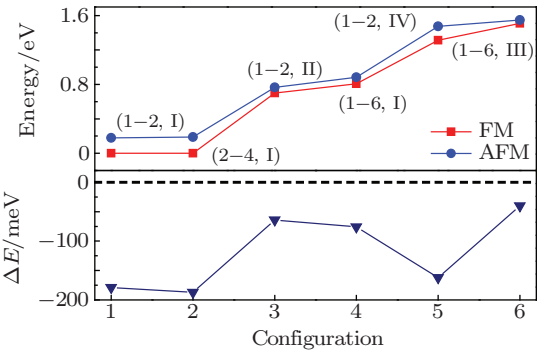


Fig. 4. (color online) Relative energies of seven different configurations with respect to that of configuration (1–2, I) in the $Zn_{34}Cu_2O_{35}N_1$ supercell. ΔE determines the magnetic stability (ΔE¡0 indicates favorable FM) of the systems.

The most stable configuration (1–2, I) with the FM ordering is 179 meV (192 meV) lower in energy than the AFM one obtained in the GGA (GGA+U). Notably, we can roughly

estimate the Curie temperature T_C value to be around 460 K (490 K) from $2\Delta E/(3nK_B)$ in the mean-field approximation, where ΔE is the energy difference between the AFM and FM arrangements in the supercell, and n denotes the number of the magnetic particles in the supercell.[26] We find that one N and two Cu ions contribute about $1.78\mu_B$ to the supercell, and the remaining magnetic moment mainly arises from the spin-polarized O ions. Moreover, once the complex of Cu–N–Cu occurs, the CuO_3N tetrahedron in wurtzite ZnO is further compressed along the bond of Cu and N, the t_2 states in the minority band is apparently delocalized at the Fermi level (Figs. 5(b) and 5(e)). Simultaneously, both No and O 2p states undergo a shifting and splitting process which results in the delocalization of N 2p and O 2p orbitals (Figs. 5(c) and 5(f)). Here, the magnetic moment of N increases from $0.34\mu_B$ ($0.38\mu_B$) to $0.48\mu_B$ ($0.55\mu_B$) in the GGA (GGA+U). Additionally, the Cu–N–Cu angle is equal to 111.47°, larger than the maximum 109° given in Ref. [27], which reported that the magnetic moment decreases with the Cu–N–Cu angle decreasing in Cu-doped GaN. However, as two substituent Cu atoms are scattered and the substituent N atom which bonds to Cu_1 is far from Cu_6, it can be confirmed that the spin-down states of Cu_1 3d overlaps with that of N 2p states significantly, while the spin-down states of Cu_6 3d are similar to that of an isolated Cu impurity on a Zn site 6, indicating that the binding of Cu and N could play an essential role in the robust magnetism of ZnO.

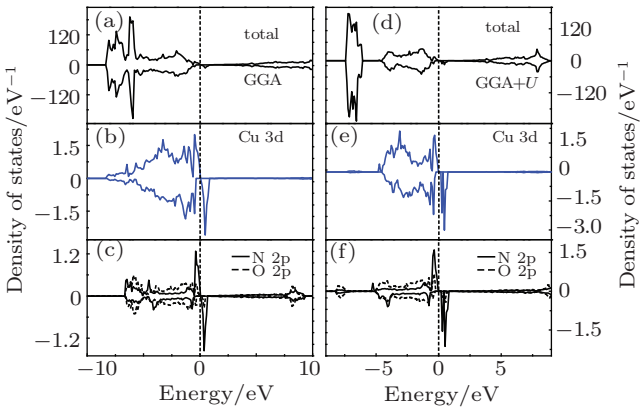


Fig. 5. (color online) (a) Total DOSs for (Cu, N)-codoped ZnO with the configuration (1–2, I) where the two nearest neighboring Zn ions are replaced by Cu, and one O ion by N. (b) Partial DOSs of Cu 3d. (c) Partial DOSs of N 2p and O 2p. Panels (d)–(f) represent the corresponding results from GGA+U calculation.

4. Conclusions

We use density-functional theory to investigate the magnetic property of (Cu, N)-codoped ZnO for various configurations. A strong tendency toward the formation of cluster is clearly observed in Cu or (Cu, N)-codoped ZnO. We conclude that the total magnetic moment mainly originates from the coexistence of the p–d hybridizations of Cu–N and Cu–O, and the p–p coupling interaction between the N 2p and O 2p states at the Fermi level. The $Zn_{34}Cu_2O_{35}N_1$ favors energetically a room temperature FM ground state which is attributed to an indirect exchange mechanism from the calculations in the GGA and GGA+U. In particular, the binding of Cu and N can play an important role in the robust magnetism of ZnO. These results suggest that the (Cu, N)-codoped ZnO is a promising dilute magnetic semiconductor free of magnetic precipitates in the field of spintronics.

References

[1] Dietl T, Ohno H, Matsukura F, Cibert J and Ferrand D 2000 *Science* **287** 1019
[2] Ohno H 2001 *Science* **291** 840
[3] Venkatesan M, Fitzgerald C B, Lunney J G and Coey M D 2004 *Phys. Rev. Lett.* **93** 177206
[4] Xiong Z H and Jiang F Y 2007 *J. Phys. Chem. Solids* **68** 1500
[5] Wang Q, Sun Q, Jena P, Hu Z, Note R and Kawazoe Y 2007 *Appl. Phys. Lett.* **91** 063116
[6] Xiong Z, Liu X C, Zhuo S Y, Yang J H, Shi E W and Yan W S 2011 *Appl. Phys. Lett.* **99** 052513
[7] Salmani E, Benyoussef A, Ez-Zahraouy H, Saidi E H and Mounkachi O 2012 *Chin. Phys. B* **21** 106601
[8] Laiho R, Ojala I and Vlasenko1 L 2010 *J. Appl. Phys.* **108** 053915
[9] Bakhtiar U H, Afaq A, Ahmed R and Naseem S 2012 *Chin. Phys. B* **21** 097101
[10] Gopal P and Spaldin N A 2006 *Phys. Rev. B* **74** 094418
[11] Tan Y S, Fang Z B, Chen W and He P Mo 2010 *Chin. Phys. B* **19** 097502
[12] Sato K, Bergqvist L, Kudrnovský J, Dederichs P H, Eriksson O, Turek I, Sanyal B, Bouzerar G, Katayama-Yoshida H, Dinh V A, Fukushima T, Kizaki H and Zeller R 2010 *Rev. Mod. Phys.* **82** 1633
[13] Zhao L, Lu P F, Yu Z Y, Guo X T, Shen Y, Ye H, Yuan G F and Zhang L 2010 *J. Appl. Phys.* **108** 113924
[14] Wang Q, Sun Q, Jena P and Kawazoe Y 2004 *Phys. Rev. B* **70** 052408
[15] Yan W S, Sun Z H, Liu Q H, Li Z R, Shi T F, Wang F, Qi Z M, Zhang G B, Wei S Q, Zhang H W and Chen Z Z 2007 *Appl. Phys. Lett.* **90** 242509
[16] Ney A, Ollefs K, Ye S, Kammermeier T, Ney V, Kaspar T C, Chambers S A, Wilhelm F and Rogalev A 2008 *Phys. Rev. Lett.* **100** 157201
[17] Pan H and Yi J B 2007 *Phys. Rev. Lett.* **99** 127201
[18] Herng T S, Qi D C, Berlijn T, Yi J B, Yang K S, Dai Y, Feng Y P, Santoso I, Hanke C S, Gao X Y, Andrew T S W, Ku W, Ding J and Rusydi A 2010 *Phys. Rev. Lett.* **105** 207201
[19] Tian Y F, Li Y F, He M, Putra I A, Peng H Y, Yao B, Cheong S A and Wu T 2011 *Appl. Phys. Lett.* **98** 162503
[20] Shen L, Wu R Q, Pan H, Peng G W, Yang M, Sha Z D and Feng Y P 2008 *Phys. Rev. B* **78** 073306
[21] Shi L B, Jin J W and Zhang T Q 2010 *Chin. Phys. B* **19** 127001
[22] Kresse G and Hafner J 1993 *Phys. Rev. B* **47** 558
[23] Perdew J P, Burke K and Ernzerhof M 1996 *Phys. Rev. Lett.* **77** 3865
[24] Decremps F, Datchi F, Saitta A M, Polian A, Pascarelli S, Cicco A D, Itié J P and Baudelet F 2003 *Phys. Rev. B* **68** 104101
[25] Puchala B and Morgan D 2012 *Phys. Rev. B* **85** 064106
[26] Hannes R, Andrés A and von Boehm1 J 2005 *Phys. Rev. B* **72** 014465
[27] Rosa A L and Ahuja R 2007 *Appl. Phys. Lett.* **91** 232109